Drug Development and Industrial Pharmacy, 2011; 37(12): 1481–1490

ISSN 0363-9045 print/ISSN 1520-5762 online
DOI: 10.3109/03639045.2011.587430

informa
healthcare

RESEARCH ARTICLE

Antitumor activity and antioxidant role of a novel water-soluble carboxymethyl chitosan-based copolymer

Mohamed El-Far[1,*], Mohamed Elshal[2], Manar Refaat[1], and Ibrahim M. El-Sherbiny[3,4,*]

[1]Biochemistry Division, Chemistry Department, Faculty of Science, Mansoura University, Mansoura, Egypt, [2]Molecular Biology Department, Genetic Engineering and Biotechnology Institute, Minoufiya University, Minoufiya, Egypt, [3]Polymer Laboratory, Chemistry Department, Faculty of Science, Mansoura University, Mansoura, Egypt, and [4]Division of Pharmaceutics, College of Pharmacy, University of Texas at Austin, Austin, TX, USA

Abstract

In this study, a natural polymer, chitosan (CS) has been converted through modified procedures to produce a water-soluble nontoxic form that has been evaluated as a novel potential antitumor drug. CS was carboxymethylated and then further modified in mild aqueous medium via graft copolymerization using a new simple and reproducible method. The synthesized new derivative of carboxymethylated CS (DCMC) was fully characterized by numerous techniques including Fourier transform infrared spectroscopy (FT-IR), elemental analyzer (EA), scanning electron microscopy (SEM), two-dimensional wide-angle X-ray scattering (2D-WAXS), and differential scanning calorimetry (DSC). The anticancer activity of the DCMC was investigated using mice bearing Ehrlich ascites tumor cells (EAC) at different doses dissolved in isotonic saline. It has been found that treatment with DCMC significantly inhibited tumor growth in a dose-dependent manner. To better understand the molecular mechanism explaining the DCMC effect on cancer cells, we tested the response of EAC cells *in vivo* to DCMC using flow cytometry cell cycle analysis. The cell cycle analysis revealed a G_2/M phase accumulation as well as a significant increase in sub-G_1 phase cells after treatment with DCMC. This indicates an induction of apoptosis in EAC cells associated with a highly significant decrease in tumor volume. In general, our results indicated that the DCMC is a regulator of tumor cell growth and differentiation not only by causing G_2/M cell cycle arrest but also inducing their apoptotic death. Moreover, the estimated hematological profile such as hemoglobin, RBCs, as well as WBCs counts revealed normal levels in mice treated with DCMC, indicating the possibility of using the DCMC in cancer chemotherapy without causing anemia like other drugs. Biochemical assays also revealed that treatment with DCMC has led to an augmentation of the antioxidant defense system without affecting lipid peroxidation in EAC-bearing mice.

Keywords: Carboxymethyl chitosan derivative, chemotherapy, tumor, apoptosis, antioxidants

Introduction

Chitosan (CS), a cationic water-insoluble polymer, has many advantageous biological properties, being biodegradable, biocompatible, nontoxic, bioabsorbable, hemostatic, bacteriostatic, fungistatic, and anticholesteremic[1,2]. Moreover, CS itself has antacid and antiulcer activities, which can prevent or weaken drug-induced irritation in the stomach[2,3]. CS also represents the core of a new generation of drug and vaccine delivery systems because of its ability to reduce the clearance rate and encourage the uptake of antigens by dendritic cells and macrophages[4–7]. In addition, the conjugates of some anticancer agents with CS and its derivatives showed promising anticancer efficiencies with a noticeable reduction in the unfavorable side effects of the original anticancer agent[4]. However, the poor solubility of CS in both water and common organic solvents limits its extensive use. Various approaches

Address for Correspondence: Ibrahim M. El-Sherbiny, Division of Pharmaceutics, College of Pharmacy, University of Texas at Austin, Austin, TX 78712, USA. E-mail: i_elsherbiny@yahoo.com (for polymer synthesis) and Mohamed El-Far, Biochemistry Division, Chemistry Department, Faculty of Science, Mansoura University, ET-35516 Mansoura, Egypt. E-mail: elfarma2002@yahoo.com (for biological assessments). Tel: +2(050) 2242-388. Fax: +2(050) 2246-254
*These authors have equally contributed to this work.

(Received 07 February 2011; revised 27 April 2011; accepted 05 May 2011)

such as carboxymethylation have been applied for conversion of CS into a water-soluble form[8]. It has been reported that carboxymethyl CS (CMCS) has several desirable characteristics including its good ability to form films, fibers, and hydrogels[9,10]. Hence, CMCS has been widely utilized in many potential applications including drug delivery[9–11].

Graft copolymerization of vinyl monomers onto polymer backbones is one of the most beneficial techniques of chemical modifications due to the ability to introduce certain desired properties via selecting appropriate types of side chains. A number of published studies have reported the graft copolymerization of vinyl monomers onto both CS[12–15] and CMCS[16–23]. This graft copolymerization onto CS and CMCS has been performed with the aid of a wide range of initiators including potassium persulfate (KPS), ammonium persulfate (APS), and ceric ammonium nitrate (CAN). These initiator systems initiate the grafting process via generating free radical sites on polymer backbones.

Grafting of acrylic acid (AA) onto CMCS, using Ce^{4+} ions as initiator, has been reported recently[18]. Also, Xie et al.[23] have synthesized the CMCS-AA copolymer with the aid of APS as initiator for investigating its antibacterial activity. In our earlier study[16], we have investigated the optimum conditions for grafting of the AA sodium salt onto CMCS backbone using APS.

The aim of this present study was to synthesize and evaluate a novel potential chemotherapeutic drug as antitumor agent. Specifically, water-soluble CMCS was synthesized and characterized. Graft copolymerization of sodium acrylate (SA) onto CMCS was then achieved with the aid of APS in mild aqueous medium. Occurrence of grafting process was confirmed by various ways. The effect of grafting on the structural characteristics of the synthesized copolymer (namely as DCMC) as compared with the starting materials was investigated with the aid of Fourier transform infrared spectroscopy (FT-IR), differential scanning calorimetry (DSC), two-dimensional wide-angle X-ray scattering (2D-WAXS), and scanning electron microscopy (SEM). Then, the potential of the newly developed copolymer (DCMC) as antitumor agent in addition to its effect on proliferation and cell cycle of cancer cells were extensively investigated. Also, some studies were performed to assess the lipid peroxidation, and antioxidant status of the developed DCMC against Ehrlich ascites carcinoma (EAC) in albino mice in addition to its effect on some vital hematological parameters.

Experimental

Materials

Anhydrous AA and APS were obtained from Aldrich (St. Louis, MO). CS was purchased from Acros Organics (Morris Plains, NJ). Monochloroacetic acid was supplied by Riedel-De Haenag Seelze (Hanover, Germany). Isopropyl alcohol, acetone, methanol, acetic acid, and all other reagents were of analytical grade and used as received.

Methods

Characterization of CS

The average molecular weight (Mw) of the CS under investigation was estimated using the Mark–Houwink viscometry method[8] in a solvent of 0.2 M NaCl/0.1 M acetic acid maintained at 25°C. The flow times of both solvent and CS solutions were determined with the aid of Cannon-Fenske Routine Viscometer (Cannon Instrument Co., State College, PA). Each sample was measured three times. The N-deacetylation% of CS was also estimated from the FT-IR analysis using the following relationship[24]:

$$\text{N-Deacetylation\%} = 100\left[\left(\frac{A_{1655}}{A_{3340}}\right)\left(\frac{1}{1.33}\right)\right] \quad (1)$$

where A is the absorbance at the given wave number. The two absorption signals at 1655 and 3340 cm^{-1} were assigned for the amide and the primary NH_2 groups of CS, respectively. The factor 1.33 is corresponding to the ratio of A_{1655}/A_{3340} for the fully N-acetylated CS.

Preparation of CMCS

The water-soluble CMCS was synthesized through a modified method as previously reported in our earlier work[8,25]. In brief, 2 g of CS were transferred to 500-mL round-bottomed flask and suspended in 50 mL of isopropyl alcohol at room temperature for 65 h. To the swollen CS suspension, 80 mL of (60% w/v) aqueous NaOH solution were added and the whole mixture was refluxed at 85°C for 2 h. Afterward, 100 mL of (60% w/v) aqueous monochloroacetic acid solution was added over a period of 15 min. The mixture was heated with stirring, at 65°C for a further 4 h. The reaction mixture was then neutralized with the aid of HCl solution (4 M). After the filtration of the undissolved residue, the produced CMCS was precipitated by adding methanol (2 volumes). The product was collected by filtration, washed several times with a mixture of methanol/H_2O (1:1), and dried at 40°C under vacuum.

The degree of substitution (D_s) of the prepared CMCS was estimated using potentiometric titration[26]. A solution of 150 mg of CMCS dissolved in 50 mL of distilled water was adjusted to pH <2 by adding HCl solution. The CMCS solution was then titrated against 0.1 M aqueous NaOH with the pH value recorded simultaneously. The NaOH amount was determined by the second-order differential method and the D_s value was calculated as follows:

$$D_s = \frac{161 \times V \times C}{m_{CMCS} - 58 \times V \times C} \quad (2)$$

where m_{CMCS} is the mass (g) of CMCS, V and C are the volume and molarity of NaOH solution, respectively. The values 161 and 58 represent the molecular weights of the

glucosamine unit of CS and the carboxymethyl group, respectively.

The average molecular weight of the CMCS, dissolved in 0.1 M aqueous NaCl, was determined at 25°C using the following set of relationships[26]:

$$\eta_r = \frac{t}{t_0}$$
$$\eta_{sp} = \eta_r - 1$$
$$[\eta] = \frac{(4\eta_{sp}^{1.02} \times \ln \eta_r)}{C^{1.01}(3\eta_{sp} + \ln \eta_r)} \quad (3)$$
$$[\eta] = 7.92 \times 10^{-5} M_r^{1.00}$$

where t_0 and t are the efflux times of the solvent and CMCS solution, respectively, C is the CMCS concentration (g/mL), η_r and $[\eta]$ are the relative and intrinsic viscosities, respectively. M_r is the viscosity average molecular weight of CMCS.

Preparation of CMCS-based graft copolymer

The free radical graft copolymerization of SA onto CMCS backbone was carried out in presence of APS as described in details in our earlier study[16]. In brief, in a 250-mL two-necked glass flask, a predetermined amount of AA monomer was converted into SA through neutralization with NaOH (4 M) and then completed to the desired volume by deionized water to give a final concentration of 1.3 mM. To the SA monomer solution, 0.1 g CMCS was added with stirring for 30 min under bubbling of slow stream of nitrogen gas. The flask was placed in a thermostated oil bath at 70°C, then the APS initiator solution (8 mM based on the total volume of reaction mixture) dissolved in 10 mL of deionized water was added dropwise with stirring. The graft copolymerization was continued for 2 h followed by stopping the reaction by letting air into the flask and rapidly cooling down the reaction. The products were precipitated by pouring the reaction mixture into acetone. The precipitate was filtered off, washed with acetone, and the crude product was dried under vacuum and weighed. The formed homopolymer (polysodium acrylate, PSA) was extensively extracted in a Soxhlet apparatus by refluxing with methanol for 24 h. The residual graft copolymer was washed with methanol, dried, and weighed. Both grafting percentage (G%) and the grafting efficiency (GE%) of the resulting CMCS grafted with SA (DCMC) copolymer were calculated according to the following relationships[27]:

$$G\% = 100[(W_g - W_0)/W_0]$$
$$GE\% = 100[W_g/(W_g + W_h)] \quad (4)$$

where W_g, W_h, and W_o are the weights of graft copolymer, homopolymer, and the starting polymer, CMCS, respectively. Both G% and GE% represent the average value ± SD of three independent grafting experiments.

Characterization

The elemental analysis for CMCS and the synthesized graft copolymer (DCMC) were performed in Carlo Erba Elemental analyzer EA 1108 using a flash combustion technique. Also, both CMCS and DCMC copolymer were characterized using FT-IR. The dried samples were pressed with spectroscopy grade KBr and their FT-IR spectra were recorded on a Perkin Elmer Paragon 1000 FT-IR spectrometer within a wave number range of 600–4000 cm^{-1} at 25°C. DSC of CMCS and DCMC copolymer were performed using Perkin Elmer DSC7 in a nitrogen atmosphere from –30°C to 300°C at a heating rate of 10°C/min. The samples (10–12 mg) were weighed into aluminium sample pans and sealed. An empty aluminium pan of approximately equal weight was used as a reference. The peaks were determined and the areas were converted into enthalpy values.

Surface morphology

The surface morphology of the dried CMCS and the graft copolymer (DCMC) was investigated by SEM (Hitachi S-800 field emission SEM operated in secondary electron mode with a Robinson backscatter detector). The digital image capture system that is used for obtaining the digital images is a Hitachi PCI system. Dry samples were mounted on aluminium stubs with double-sided conducting carbon tapes and coated with a 50/50 mixture of gold and palladium to minimize surface charging. The sample was scanned at an accelerating voltage of 20 kV.

2D-X-ray analysis

The WAXS of CS, CMCS, and DCMC copolymers were investigated using 2D-WAXS equipment (Rigaku Micro Max 007 microfocus imitating anode X-ray generator (Cu Kα) coupled with Osmic "Blue" confocal optics and a Rigaku RAxis (VI++) image-plate detector. Images were recorded and analyzed with Crystal Clear (1.3.6-SPI, Pflugrath, JW, 1999, Acta Crystallogr. D50 1718–1725)[28].

The d-spacing values of the investigated molecules in the crystalline, semicrystalline, and amorphous states were calculated from the scattering wave vector q (=$(4\pi/\lambda)\sin\theta$, where 2θ is the scattering angle) according to the following relationship:

$$d = \frac{2\pi}{q} \quad (5)$$

Tumors and biochemical protocols

The newly developed CS derivative (DCMC) was dissolved using isotonic saline solution and diluted to the desired concentration. All experiments were performed with adult Swiss albino mice strain purchased from Theodore Bilharz institute, Giza, Egypt, with an average body weight of 20 to 25 g. Mice were housed in steel mesh cages and maintained for 1 week acclimatization periods

on commercial standard diet and tap water *ad libitum*. EAC line was kindly supplied from the National Cancer Institute, Cairo University, Egypt.

Tumor cells and transplantation of EAC cells

EAC cells were used for *in vivo* experiments. The tumor cell line was maintained in mice through serial intraperitoneal (i.p.) transplantations of (2×10^6) viable tumor cells in 0.2 mL of saline using a 25 G needle. The tumor was characterized by moderately rapid growth, while killing mice within 3 weeks due to accumulation of ascetic fluid and showing no distal metastasis or spontaneous regression. Counting of the viable EAC cells was carried out by trypan blue exclusion using the method described[29].

In vivo *antitumor activity and tumor volume experiments*

Swiss albino female mice were divided to several groups, five mice in each cage at least. All animals were housed in plastic cages and maintained under controlled conditions of humidity, temperature, and normal environment of light and darkness. Animals were randomly assigned to several groups as follows: Group 1 ($n = 10$) animals were injected (i.p.) with 0.2 mL of EAC cells containing 1×10^6 cells for tumor induction and then left without any treatment for 14 days (control a). Group 2 ($n = 10$) animals were injected (i.p.) with 0.2 mL of EAC cells containing 2×10^6 cells for tumor induction and then left without any treatment for 14 days (control b). Group 3 ($n = 5$) animals were injected (i.p.) with 0.2 mL of EAC cells containing 1×10^6 cells, next day animals received DCMC (i.p.) at a dose of 25 mg/kg body weight dissolved in 0.2 mL isotonic saline day after day for 14 days (six separate doses). After 18 h of the last dose administration, the mice were then sacrificed for observation of antitumor activity and then compared with that obtained in the same way in mice of control a. Group 4 ($n = 5$) animals were injected (i.p.) with 0.2 mL of EAC cells containing 2×10^6 cells, next day animals received DCMC (i.p.) at a dose of 50 mg/kg body weight dissolved in 0.2 mL isotonic saline day after day for 14 days (six separate doses). After 18 h of the last dose administration, the mice were subjected to antitumor activity evaluation by comparing it with the control b group. Group 5 ($n = 5$) animals were injected (i.p.) with 0.2 mL of EAC cells containing 2×10^6 cells, next day animals received DCMC (i.p.) at a dose of 100 mg/kg body weight dissolved in 0.2 mL isotonic saline day after day (i.e. every 48 h) for 14 days (six separate doses). After 18 h of the last dose administration, the mice were subjected to antitumor activity evaluation by comparing it with control b group. The effect of the tested synthesized compound DCMC on the growth of transplantable murine tumor, and simultaneous alterations in hematological profile were estimated according to El-Far et al.[30,31] The antitumor effect was assessed by observation of changes with respect to ascetics tumor volume. Hemoglobin (Hb) content, red blood cells (RBCs), and white blood cells (WBCs) were estimated from the blood collected from each group of animals using autoanalyzer at Mansoura University Hospital.

Flow cytometry protocol

This was determined in cells collected from nontreated and tumor-bearing treated groups of animals according to El-Far et al.[31] In brief, cells were fixed in 70% ice cold ethanol. Cells were washed prior to analysis using phosphate-buffered saline (PBS) (pH 7.4), and incubated with RNAse A (100 μg/mL) and the DNA-intercalating dye propidium iodide (20 μg/L) in citrate buffer (3.4 mM). Cell cycle analysis including DNA content, DNA index, cellular proliferation, and apoptosis were measured using FACSCalibur (Becton Dickson, Mountain View, CA) and Cellquest software (Becton Dickson) with an excitation wavelength of 488 nm and emission above 580 nm. The cell cycle analysis was performed using Mod-Fit software. Fifteen thousand cells were analyzed in each experiment.

Apoptosis detection in EAC cells

Cells were fixed and stained with propidium iodide and DNA content was revealed by flow cytometry, with apoptotic cells forming a sub-G_1 peak. As a negative control, a sample with live cells was used. Up to 15,000 cells were analyzed using the Cellquest software.

Estimation of biochemical parameters

After the collection of ascetic samples from the groups of mice, EAC cells were homogenized with cold saline solution using a homogenizer, and then the biochemical parameters were estimated. The levels of malondialdehyde (MDA) were estimated in cell homogenate according to Ohkawa et al.[32] The levels of nitric oxide (NO) and superoxide dismutase (SOD) were also determined according to Green et al.[33] and Dechatelet et al.[34], respectively.

Statistical significance

All values were expressed as mean ± SD. The statistical significance was determined using the one-way ANOVA. Statistical package for social science (SPSS, Inc., Chicago, IL) was used for the statistical analysis. Statistical significance was considered at values of $P < 0.05$, whereas highly significance was considered at values of $P < 0.001$.

Results and discussion

Characterization of CS, CMCS, and the graft copolymer (DCMC)

The average Mw of the CS utilized in the current study was estimated to be 318 kDa using the Mark–Houwink viscometry method[8]. Also, the N-deacetylation% of the CS was found to be 73.6% as determined by FT-IR[24]. The D_s value of the prepared CMCs was found to be 0.48 as determined by potentiometric titration and its intrinsic viscosity in 0.1 M aqueous NaCl at 25°C was found to be 5.1 dL/g. The grafting yield (G% and GE%) of the

resulting copolymer (DCMC) was estimated gravimetrically according to Equation 4 and found to be 2900% and 37.2%, respectively. The structural differences between the starting polymer, CS and its derivatives, CMCS, and DCMC were confirmed with the aid of FT-IR as apparent in Figure 1. In the case of CS, the FT-IR spectrum (Figure 1a) revealed a strong signal at 3427 cm^{-1}, which was attributed to the O–H stretching vibration, N–H extension vibration, and the intermolecular H-bonds of the polysaccharide moieties. The weak signal appeared at 1654 cm^{-1} was attributed to the amide C=O stretching vibration. The FT-IR spectrum of CMCS (Figure 1b) demonstrated a strong new peak at 1734 cm^{-1} representing the carboxylate C=O asymmetric stretching vibration. The peak appeared at 1384 cm^{-1} could be assigned to the symmetric stretching vibration of carboxylate C=O group. The C–O absorption signal of the secondary hydroxyl group became stronger and has been shifted to 1089 cm^{-1}. This tends to indicate that the substitution occurred particularly at the C_6 position of the CS backbone. In the FT-IR spectrum of the copolymer, DCMC (Figure 1c), the absorption signal appeared at 1319 cm^{-1} is characteristic of the homopolymer, poly(SA). Also, in the FT-IR spectrum of the graft copolymer, the characteristic absorption signals of the polysaccharide moieties at around 1100 cm^{-1} became weaker and that can be attributed to the relatively high grafting percentage. The FT-IR spectrum of the copolymer, DCMC, also revealed the absence of clear absorption due to vinyl unsaturation around 1640 cm^{-1}. This tends to indicate the disappearance of the vinylic double bond of SA monomer due to the grafting process. Several literature reports showed that the initiation site in this type of free radical-induced graft copolymerization reactions onto CMCS backbone is the primary NH_2 groups on the C_2 position[35] as illustrated in Scheme 1.

The incidence of graft copolymerization of the SA monomer onto CMCS backbone was confirmed by various methods. For example, the higher weight of the produced graft copolymer as compared with that of the starting polymer, CMCS, after the extensive removal of the homopolymer, poly(SA), can be considered an evidence of grafting. Also, the FT-IR spectra of the synthesized DCMC copolymer as discussed above showed both characteristic peaks of the CMCS and SA. This can be taken as another experimental evidence of grafting process. Occurrence of grafting was also deduced from the decreasing of the N-content upon comparing the elemental analysis data of both CMCS and the prepared DCMC copolymer as apparent in Table 1.

Structural study of DCMC copolymer

Wide-angle X-ray scattering

The 2D-WAXS analysis of the powder samples were performed by using X-ray beam with a double graphite monochromator for the CuKα radiation (λ = 0.154 nm). Figure 2 illustrates some typical patterns for the investigated polymer molecules, CMCS, DCMC, and poly(SA).

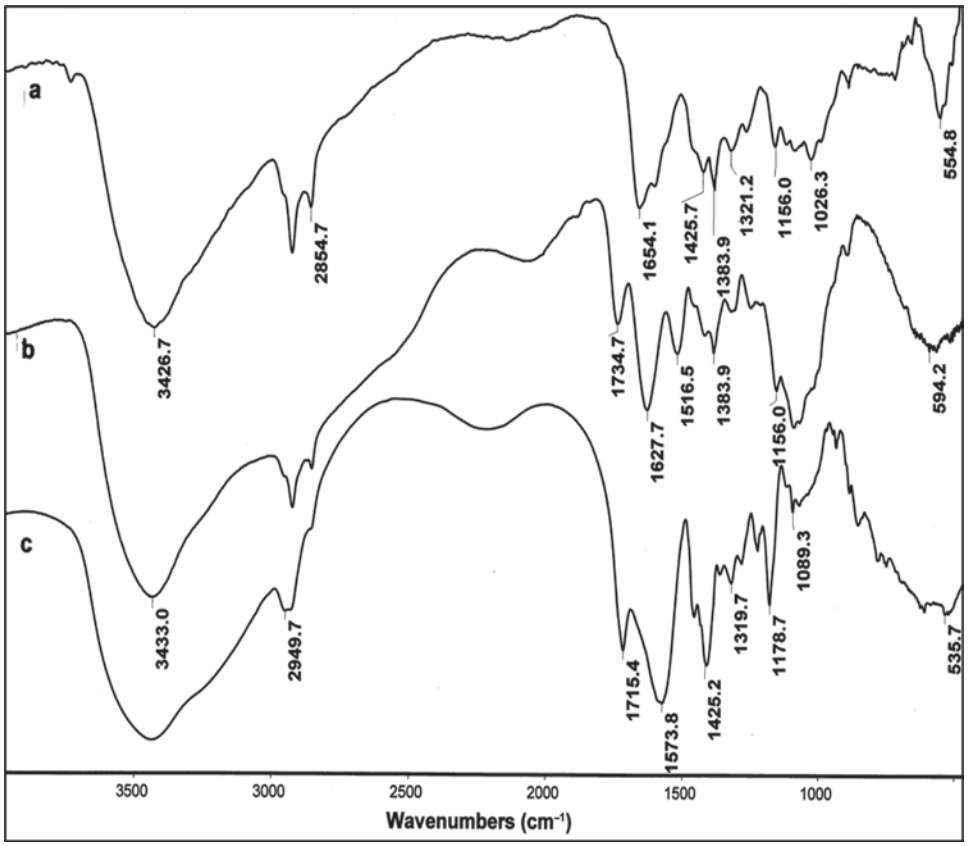

Figure 1. Fourier transform infrared (FT-IR) spectra for (a) CS, (b) CMCS, and (c) DCMC copolymer.

The 2D-WAXS patterns shown in Figure 2 demonstrated that CMCS (Figure 2A) has many crystalline peaks in addition to two weak bands corresponding to 2θ values of about 8.6° and 6.4°. Grafting of SA onto the CMCS backbone turned the resulting copolymer, DCMC, into an amorphous material (Figure 2B). The diffractogram of the copolymer showed some weak peaks at 2θ values of 11.9° and 4.1°. This resulting amorphous structure of the synthesized graft copolymer, DCMC, can be attributed to occurrence of grafting in a random manner along the polymer backbone and consequently destroying regularity of packing of the original polymer chains leading to formation of amorphous structure. The diffractogram of the poly(SA), as a reference, showed a mostly amorphous nature of it. Comparing the diffraction patterns of the synthesized DCMC copolymer with those of CMCS and poly(SA) can also be taken as additional evidence of occurrence of the grafting process. The 2θ values as well as the calculated *d*-spacing of the investigated polymer molecules are shown in Table 1.

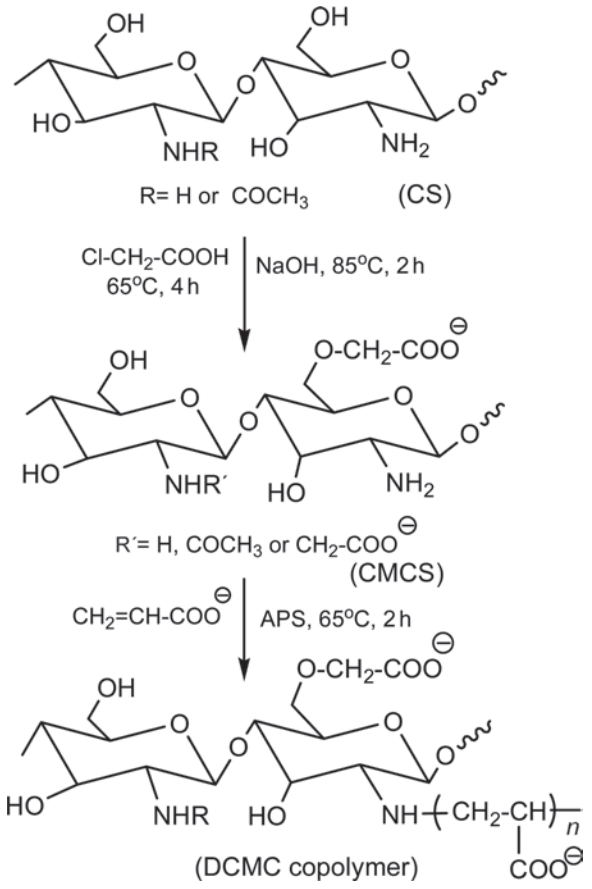

Scheme 1. Preparation of the DCMC graft copolymer.

Differential scanning calorimetry

The traces from the second heating run for CMCS and DCMC copolymer in the temperature range from 243 to 573 K are illustrated in Figure 3. An obvious step in the specific heat can be noted at the glass transition temperature (T_g). The T_g was determined as the temperature of the midpoint of the heat capacity increment in the transition. The specific heat (Δc_p) and T_g of the investigated polymer molecules are shown in Table 1.

As apparent from the figure, the thermal behavior of both CMCS and DCMC copolymer revealed the absence of a phase transformation within the investigated *T*-range. However, a clear step in the specific heat can be seen at the glass temperature (T_g). Also, an abrupt change in the value of the heat capacity step (Δc_p) of the nongrafted polymer (CMCS) can be noted upon grafting (see Table 1). Moreover, from the DSC data, the increase of the T_g upon grafting indicates that the CMCS backbone became more rigid due to the attachment of the SA side chains, which led to a slowdown in mobility of the main CMCS chains.

Surface morphology

The surface morphology of the DCMC copolymer as compared with the CMCS is shown in Figure 4. As apparent from the figure, the grafting process has turned the rough and irregular clusters of CMCS into a different morphology with appearance of some microcrystalline aggregates, which can be attributed to the grafted poly(SA) side chains.

In vivo evaluation of the antitumor activity of DCMC

The antitumor activity was evaluated on EAC-bearing mice using animal model. The synthesized DCMC (G% 2900%) at a dose level of 25 mg/kg showed highly significant decrease in tumor volume at the end of *in vivo* experiment when compared with EAC control nontreated (a) group at the same experimental conditions, using 1 million of cells for tumor induction (Table 2 and Figure 5).

The DCMC at dose levels of 50 and 100 mg/kg injected to EAC-bearing mice that received 2 millions of cells for tumor induction showed that reduction of tumor volume is a dose-dependent as compared with that of EAC control nontreated group (b) at the same experimental conditions of using 2 millions of cells for tumor induction

Table 1. Some characteristics of the prepared CMCS, poly(SA), and the DCMC copolymer molecules.

Sample code	G%	Elemental analysis data				Δc_p ($Jg^{-1}K^{-1}$)	T_g (K)	XRD data for the investigated molecules		
		C (%)	N (%)	H (%)	O (%)			*d* (nm)	2θ (°)	Phase
CMCS	—	37.21	5.11	5.85	51.83	11.88	481.64	0.20, 2.01, 2.21, 2.93, 3.18	45, 8.50, 6.44, ~5.5, 4.41, ~3.98, 3.21, 3.04, 2.82	Semicrystalline
DCMC	2900	37.40	0.13	4.78	57.69	0.75	499.65	0.74, 2.16	11.9, 4.1	Amorphous
Poly(SA)	—	49.91	—	5.71	44.38	—	—	2.02	4.4	Highly amorphous

(Table 3). Also, as apparent from Table 3, a highly significant decrease in tumor volume was observed at dose level of 100 mg/kg.

In cancer chemotherapy, one of the major problems is anemia, which is mainly due to reduction of RBCs or hemoglobin percentage. Treatment with our new water-soluble copolymer, DCMC, retained the Hb content, RBCs, and also the WBCs count at normal levels when compared with control group (Table 4). Furthermore, none of the treated mice with our new investigated compound exhibited any abnormal behavior or any toxicity symptoms at doses used during this study, which indicated the safety of its use as antitumor compound. It is worth mentioning that storage of this synthesized material is very important. Different results have been obtained upon using the DCMC material after storage at room temperature for >6 months. The DCMC color turned yellowish and when tested on animals they showed some symptoms of toxicity at higher doses, with loss of appetite and dizziness. This behavior may be attributed to occurrence of partial hydrolysis of the DCMC either in the main polysaccharide CMCS backbone or in the side chains of the DCMC graft copolymer leading to the production of some poly(SA) impurities.

The effect of the developed DCMC copolymer on the lipid peroxidation was also investigated as illustrated in Tables 2 and 3 by the determination of the levels of MDA in mice treated with DCMC and EAC. As apparent from the data, there was no significant change observed in the values and all the values were found to be within the normal range. This tends to indicate the absence of any harmful lipid peroxidation effect upon using the DCMC copolymer.

Due to the significant role played by the increased NO levels in human diseases[36,37], the NO levels in most of the animals treated with the developed DCMC were estimated and were found to be within the normal range when compared with EAC-bearing control animals (Tables 2 and 3). On the other hand, the levels of the enzyme, SOD in mice treated with DCMC revealed a highly significant increase upon using DCMC in a dose-dependent manner as compared with that of the EAC control group (Tables 2 and 3). The SOD is a free radical scavenging and it provides a defense against the potentially damaging reactivity of superoxide and hydrogen peroxide[37,38]. From the data in Tables 2 and 3, the administration of DCMC has increased significantly the levels of SOD, which indicates the antioxidant and free radical scavenging characteristics of DCMC. It is well-known that the excessive production of free radicals would lead to an oxidative stress, which causes damage of macromolecules such as lipids and induces lipid peroxidation *in vivo*[37,38]. The MDA, the end product of lipid peroxidation, was reported to be increased in cancer tissues. Our data showed that the

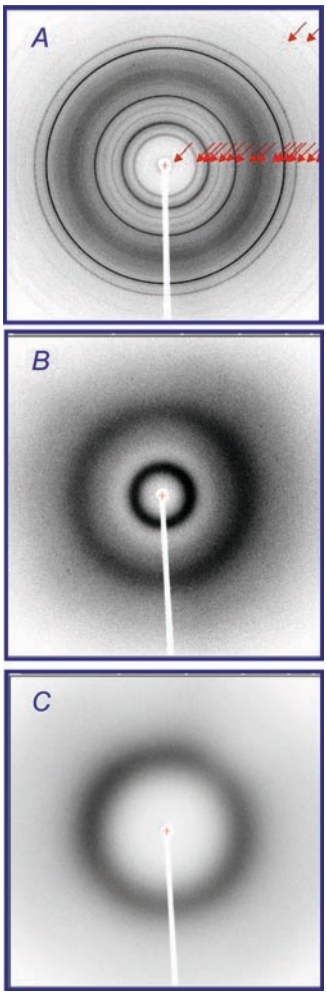

Figure 2. Two-dimensional wide-angle X-ray scattering (2D-WAXS) images, taken at $T = 298$ K, of the (A) CMCS, (B) DCMC copolymer (G%, 2900), and (C) poly(SA).

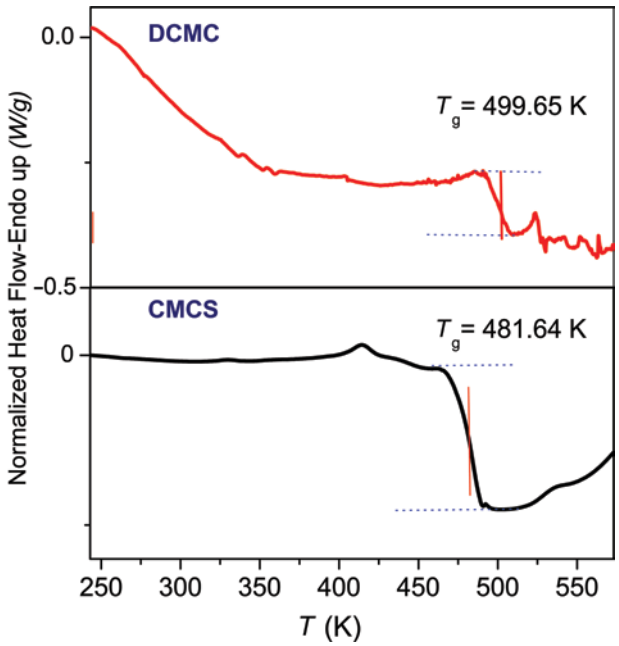

Figure 3. Differential scanning calorimetric (DSC) thermograms of the synthesized DCMC in comparison with that of the starting polymer, CMCS obtained during the second heating runs with a rate of 10 K/min. The vertical lines indicate the respective glass transition temperature.

administration of DCMC did not increase the MDA and significantly increased the SOD activity. This indicates that the DCMC has a potential as antitumor agent with an inhibition ability of EAC-induced intracellular oxidative stress with additive antioxidant activity; however, further investigations are still needed.

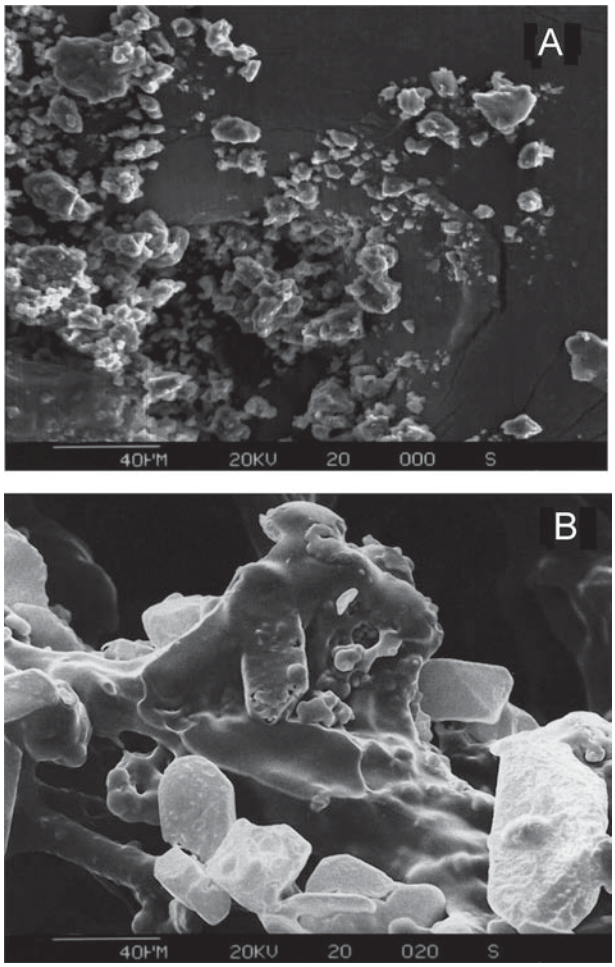

Figure 4. Scanning electron micrographs of (A) CMCS and (B) DCMC copolymer.

Flow cytometry

The flow cytometry results are summarized in Table 5. As apparent from the table, the effect of the synthesized compound, DCMC, on apoptosis (sub-G_1) of EAC was found to be dose-dependent. The concentration of 100 mg/kg has induced a significant apoptosis, which is in agreement with the highly significant decrease observed in tumor volume at the same experimental conditions (Table 3). The obtained results also indicated that depletion of G_0/G_1 might indicate that the cell death and especially apoptosis is induced from G_0/G_1 phase of the cell cycle after treatment with 100 mg/kg of DCMC. On the other hand, the DNA synthesis analyzed by flow cytometry revealed nonsignificant changes with all the various concentrations used when

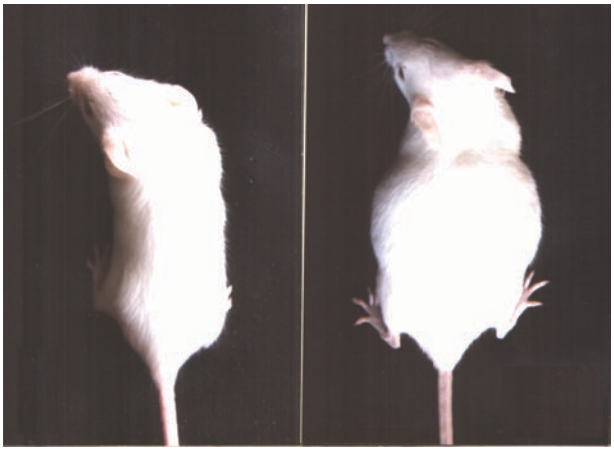

Figure 5. Effect of DCMC at dose 25 mg/kg body weight on mice with Ehrlich ascites carcinoma (EAC) (left), compared with an EAC control nontreated animal (right). Substantial difference observed on treated animals.

Table 2. Tumor volumes, levels of malondialdehyde (MDA), levels of nitric oxide (NO), and the levels of superoxide dismutase (SOD) in mice treated with DCMC (with dose of 25 mg/kg, day after day for 2 weeks) compared with control nontreated tumor-bearing group using 1 million of cells/mouse.

Groups	Tumor volume (mL) ± SD	MDA(nmol/g wet tissue) ± SD	NO (μmol/L) ± SD	SOD (% of inhibition) ± SD
EAC Control ($n=10$)	2.73 ± 0.25	31.38 ± 4.3	27.00 ± 3.24	23.14 ± 5.11
DCMC ($n=5$)	1.32 ± 0.21**	32. 14 ± 5.42	28.40 ± 3.57	28.95 ± 4.91*

(*) significant, $P > 0.05$; (**) highly significant, $P > 0.001$ for effect on treated groups versus the control group. All the values in the table represent mean ± SD.

Table 3. Tumor volumes, levels of malondialdehyde (MDA), levels of nitric oxide (NO), and the levels of superoxide dismutase (SOD) in mice treated with DCMC (with dose of 50 and 100 mg/kg, day after day for 2 weeks) compared with control nontreated tumor-bearing group using 2 millions of cells/mouse.

Groups	Tumor volume (mL) ± SD	MDA(nmol/g wet tissue) ± SD	NO (μmol/L) ± SD	SOD (% of inhibition) ± SD
EAC Control ($n=10$)	4.13 ± 0.61	31.38 ± 4.35	27.10 ± 3.24	23.14 ± 5.11
DCMC 50 ($n=5$)	4.20 ± 0.57	32.23 ± 4.78	25.40 ± 6.10	29.46 ± 6.00*
DCMC 100 ($n=5$)	2.60 ± 0.41**	32.40 ± 5.01	21.60 ± 3.78*	36.83 ± 6.44**

(*) significant, $P > 0.05$; (**) highly significant, $P > 0.001$ for effect on treated groups versus the control group. All the values in the table represent mean ± SD.

Table 4. Hemoglobin, levels of red blood cells (RBCs), and levels of white blood cells (WBCs) in mice treated with DCMC (with dose of 25 mg/kg, day after day for 2 weeks) compared with control nontreated tumor-bearing group using 1 million of cells/mouse.

Groups	Hb/g% ± SD	RBCs ($\times 10^6$/μL) ± SD	WBCs ($\times 10^3$/μL)± SD
EAC Control ($n=5$)	12.74 ± 3.28	9.31 ± 2.52	11.6 ± 3.85
DCMC ($n=5$)	11.76 ± 1.53	8.28 ± 2.31	10.08 ± 1.77

(*) significant, $P > 0.05$; (**) highly significant, $P > 0.001$ for effect on treated groups versus the control group. All the values in the table represent mean ± SD.

Table 5. Flow cytometric analysis of Ehrlich ascites carcinoma (EAC) cells.

Group	No.	Sub-G_1	SD	G_0/G_1	SD	S-phase	SD	G_2/M	SD
Control	4	5.6	1.2	46.2	7.9	25.5	8.2	15.7	3.8
DCMC, 25 mg/kg/day	7	7.2	2.1	51	4.6	22.3	1.9	19.7	2.1
DCMC, 50 mg/kg/day	6	6.4	3.3	44.5	6.1	23.1	2.5	25.9	1.4
DCMC, 100 mg/kg/day	3	11.3*	3.6	41.6	12.3	19	5.4	33.4*	9.7

*P-value <0.05 in comparisons with untreated control group values.

compared with untreated control group. More interestingly, the treatment with DCMC showed a significant increase in G_2/M phase in a dose-dependent way, which is also in agreement with the data that revealed a highly significant decrease in tumor volume at high dose (Table 3). The present study has also shown that DCMC has potent anticarcinogenic and proapoptotic effects in EAC cells *in vivo*. We have examined whether DCMC can also inhibit angiogenesis and induce apoptosis in the EAC cell lines in a dose-dependent manner. EAC cells treated with DCMC acquired apoptotic morphological features as well as increased apoptotic percentage as detected in the forms of increase in the sub-G_1 phase of the cell cycle using flow cytometry associated with a decrease in G_0/G_1 phase. These data are in the same line with the worldwide accepted opinion that apoptosis is induced from G_0/G_1 phase[40]. Also, our results concerning the increase in apoptotic percentage are in agreement with the finding of Prashanth and Haranathan that depolymerized products of CS are inhibiting the growth of EAC in mice due to induction of apoptosis[41]. Moreover, the DCMC has induced arrest in the G_2/M phase which was shown to be a dose-dependent process.

The G_2/M checkpoint is currently receiving growing attention as a target for cancer therapeutics. The G_2/M checkpoint prevents cells from attempting to undergo mitosis in an inappropriate state and due to defects in G_1 checkpoint mechanisms, cancer cells depend on G_2/M checkpoint far more than normal cells suggesting that therapeutic agents acting at this cell cycle phase may confer tumor selectivity. The induction of apoptosis as reflected from the significant increase in apoptotic cells that form sub-G_1 phase (Table 5), and the accumulation of cells in G_2/M checkpoint may account for the inhibition of cancer cell growth upon the administration of the DCMC. This study, therefore, suggests DCMC as a G_2/M checkpoint regulator, arresting cells in this stage of the cell cycle and inducing their apoptotic death. Therapeutic agents targeting the G_2/M checkpoint emerged as a new and potentially targeted approach to cancer and further extensive study of DCMC derivatives is eagerly awaited. In particular, evaluation of its efficacy in noncancerous cells would indicate its tumor selectivity. Also, further studies in cells harboring P53 mutation will be conducted.

Conclusion

The results of this current study illustrated that the synthesized new CMCS-based copolymer (DCMC) has significantly inhibited the tumor growth. The response of EAC cells *in vivo* to DCMC was tested using flow cytometry cell cycle analysis and the data showed a G_2/M phase accumulation plus induction of apoptosis in EAC cells associated with a highly significant decrease in tumor volume. The results indicated that the DCMC acts also as a regulator of tumor cell growth and differentiation causing G_2/M cell cycle arrest and inducing their apoptotic death. Hematological profile depicted normal levels in the mice treated with DCMC, indicating a potential for the use of DCMC in cancer chemotherapy without causing anemia like other available drugs. Moreover, the biochemical assays showed that the treatment with DCMC led to augmentation of antioxidant defense system without affecting lipid peroxidation in EAC-bearing mice. In conclusion, the collected data reveal a very promising potential for the investigated compound, DCMC, as anticancer agent and the efficacy of some other DCMC derivatives as anticancer agents is currently under extensive investigation by our group.

Declaration of interest

The authors report no declarations of interest.

References

1. Muzzarelli RA, Mattioli-Belmonte M, Pugnaloni A, Biagini G. (1999). Biochemistry, histology and clinical uses of chitins and chitosans in wound healing. In: Chitin and Chitinases (Jolles P, Muzzarelli RAA, Eds.), Birkhauser, Basel, p. 251.
2. Hou WM, Miyazaki S, Takada M, Komai T. (1985). Pharmaceutical application of biomedical polymers. Part XVI. Sustained release of indomethacin from chitosan granules. Chem Pharm Bull, 33:3986.

3. Miyazaki S, Ishii K, Nadai T. (1981). The use of chitin and chitosan as drug carriers. Chem Pharm Bull, 29:3067–3069.
4. Kato Y, Onishi H, Machida Y. (2003). Application of chitin and chitosan derivatives in the pharmaceutical field. Curr Pharm Biotechnol, 4:303–309.
5. Kim MS, Sung MJ, Seo SB, Yoo SJ, Lim WK, Kim HM. (2002). Water-soluble chitosan inhibits the production of pro-inflammatory cytokine in human astrocytoma cells activated by amyloid beta peptide and interleukin-1beta. Neurosci Lett, 321:105–109.
6. Marcinkiewicz J, Polewska A, Knapczyk J. (1991). Immunoadjuvant properties of chitosan. Arch Immunol Ther Exp (Warsz), 39:127–132.
7. Maeda M, Murakami H, Ohta H, Tajima M. (1992). Stimulation of IgM production in human—human hybridoma HB4C5 cells by chitosan. Biosci Biotechnol Biochem, 56:427–431.
8. El-Sherbiny IM. (2009). Synthesis, characterization and metal uptake capacity of a new carboxymethyl chitosan derivative. Euro Polym J, 45:199–210.
9. Chen L, Du Y, Tian Z, Sun L. (2005). Effect of the degree of deacetylation and the substitution of carboxymethyl chitosan on its aggregation behavior. J Polym Sci Polym Phys, 43:296–305.
10. Muzzarelli RAA. (1988). Carboxymethylated chitins and chitosans. Carbohyd Polym, 8:1–21.
11. Liu Z, Jiao Y, Zhang Z. (2007). Calcium–carboxymethyl chitosan hydrogel beads for protein drug delivery system. J Appl Polym Sci, 103:3164–3168.
12. Li YP, Liu L, Fang YE. (2003). Plasma-induced grafting of hydroxyethyl methacrylate (HEMA) onto chitosan membranes by a swelling method. Polym Int, 52:285–290.
13. Radhakumary C, Divya G, Nair PD, Mathew S, Nair CPR. (2003). Graft copolymerization of 2-hydroxyethyl methacrylate onto chitosan with cerium (IV) ion. I. Synthesis and characterization. J Macromol Sci A, 40:715–730.
14. Jenkins DW, Hudson SM. (2002). Heterogeneous graft copolymerization of chitosan powder with methyl acrylate using trichloroacetyl-manganesecarbonylco-initiation. Macromolecules, 35:3413–3419.
15. Liu YH, Liu ZH, Zhang YZ, Deng KL. (2002). Graft copolymerization of methyl acrylate onto chitosan initiated by potassium diperiodatonickelate (IV). J Macromol Sci A, 39:129–143.
16. El-Sherbiny IM, Elmahdy MM. (2010). Preparation, characterization, structure, and dynamics of carboxymethyl chitosan grafted with acrylic acid. J Appl Polym Sci, 118:2134–2145.
17. Jigar MJ, Sinha VK. (2007). Ceric ammonium nitrate induced grafting of polyacrylamide onto carboxymethyl chitosan. Carbohyd Polym, 67:427–435.
18. Joshi, JM, Sinha VK. (2007). Study of the effect of reaction variables on grafting of acrylic acid onto carboxymethyl chitosan. Designed Monom Polym, 10:207–219.
19. Joshi JM, Sinha VK. (2006). Synthesis and characterization of carboxymethyl chitosan grafted methacrylic acid initiated by ceric ammonium nitrate. J Polym Res, 13:387–395.
20. Joshi JM, Sinha VK. (2006). Graft copolymerization of 2-hydroxyethylmethacrylate onto carboxymethyl chitosan using CAN as an initiator. Polymer, 47:2198–2204.
21. Zhu A, Zhang M, Zhang Z. (2004). Surface modification of ePTFE vascular grafts with *O*-carboxymethylchitosan. Polym Int, 53:15–19.
22. Sun T, Xu P, Liu Q, Xue J, Xie W. (2003). Graft copolymerization of methacrylic acid onto carboxymethyl chitosan. Euro Polym J, 39:189–192.
23. Xie W, Xu P, Wang W, Liu Q. (2002). Preparation of water-soluble chitosan derivatives and their antibacterial activity. J Appl Polym Sci, 85:1357–1361.
24. Roberts GAF. (1992). Solubility and solution behaviour of chitin and chitosan. In: Chitin Chemistry (Roberts GAF, Ed.), MacMillan, Houndmills, pp. 274.
25. El-Far MA, Elshal MA, El-Sherbiny IM. (2009). Chemically modified chitosan as an anticancer agent. Date Lodged: November 1, 2007. Publication Number GB2454221, UK Intellectual property Office.
26. Ge HC, Luo DK. (2005). Preparation of carboxymethyl chitosan in aqueous solution under microwave irradiation. Carbohydr Res, 340:1351–1356.
27. Shantha KL, Bala U, Panduranga RK. (1995). Tailor- made chitosans for drug delivery. Euro Polym J, 31:317–382.
28. Pflugrath JW. (1999). The finer things in X-ray diffraction data collection. Acta Cryst, D55:1718 -1725.
29. McLimans WF, Davis EV, Glover FL, Rake GW. (1957). The submerged culture of mammalian cells; the spinner culture. J Immunol, 79:428–433.
30. El-Far M, Elmegeed GA, Eskander EF, Rady HM, Tantawy MA. (2009). Novel modified steroid derivatives of androstanolone as chemotherapeutic anti-cancer agents. Eur J Med Chem, 44:3936–3946.
31. El-Far M, El-Shal M, Bondocck S, Refaat M. (2009). Preclinical biochemical studies using a novel 5-aminolevulinic acid ester derivative with superior properties for photodynamic therapy of tumors. Int J Med Med Sci, 1:278–287.
32. Ohkawa H, Ohishi N, Yagi K. (1979). Assay for lipid peroxides in animal tissues by thiobarbituric acid reaction. Anal Biochem, 95:351–358.
33. Green LC, Wagner DA, Glogowski J, Skipper PL, Wishnok JS, Tannenbaum SR. (1982). Analysis of nitrate, nitrite, and [^{15}N] nitrate in biological fluids. Anal Biochem, 126:131–138.
34. DeChatelet LR, McCall CE, McPhail LC, Johnston RB Jr. (1974). Superoxide dismutase activity in leukocytes. J Clin Invest, 53:1197–1201.
35. Sabaa MW, Mohamed NA, Mohamed RR, Khalil NM, Abd El Latif SM. (2010). Synthesis, characterization and antimicrobial activity of poly (*N*-vinyl imidazole) grafted carboxymethyl chitosan. Carbohyd Polym, 79:998–1005.
36. El-Far M, El-Sayed IH, El-Motwally Ael-G, Hashem IA, Bakry N. (2007). Tumor necrosis factor-alpha and oxidant status are essential participating factors in unexplained recurrent spontaneous abortions. Clin Chem Lab Med, 45:879–883.
37. El-Far M, El-Motwally Ael-G, Hashem IA, Bakry N. (2009). Biochemical role of intravaginal sildenafil citrate as a novel antiabortive agent in unexplained recurrent spontaneous miscarriage: first clinical study of four case reports from Egypt. Clin Chem Lab Med, 47:1433–1438.
38. El-Far M, El-Sayed IH, El-Motwally A, Hashem I, Bakry N. (2009). Analysis of some antioxidant enzymes combined with the detection of TNF-α expression in unexplained recurrent spontaneous abortion: correlations with LH and FSH hormones. J Physiol Biochem, 65:175–182.
39. Yagi K. (1987). Lipid peroxides and human diseases. Chem Phys Lipids, 45:337–351.
40. Darzynkiewicz JS, Li X, Gorczyca W et al. (1997). Cytometry in cells necrobiology: analysis of apoptosis and accidental cell death (necrosis). Cytometry, 27:1–20.
41. Harish Prashanth KV, Tharanathan RN. (2005). Depolymerized products of chitosan as potent inhibitors of tumor-induced angiogenesis. Biochim Biophys Acta, 1722:22–29.